Available online at www.sciencedirect.com
ScienceDirect
Cement and Concrete Research 37 (2007) 231–241
Cement and Concrete Research

Aspects of moisture kinetics of coal bottom ash in concrete

L.B. Andrade, J.C. Rocha *, M. Cheriaf

Department of Civil Engineering, Federal University of Santa Catarina, Florianópolis-SC, 88040-900, Brazil

Received 20 July 2005; accepted 2 November 2006

Abstract

The moisture kinetics aspects of composite granular material samples composed of natural sand and bottom ash (BA) from thermoelectric power stations and the use of this material in the production of durable concretes, in relation to water transport, are here discussed. The evaluations of the phenomenon of water absorption by capillarity and the loss of water through air drying until hygroscopic equilibrium, were carried out in accordance with classic procedures found in the literature and also newly developed procedures. The results showed that due to the high porosity of BA, the water absorption by capillarity along with the absorption velocity were higher in the compositions with greater BA content. The values for moisture equilibrium from air drying, absorption from capillarity and sorptivity obtained in the hygroscopic equilibrium tests, carried out on the same samples after absorption, were also higher in the samples with BA. These samples also requited a longer drying time.

Keywords: Bottom ash; Coal; Concrete; Moisture; Drying; Capillarity

1. Introduction

The use of by-products or wastes from coal-fired thermoelectric power plants has evolved into a reality in the production of concrete, resulting in good mechanical performance, good compatibility with raw materials in the concrete and durability [1–3].

The use of fly ash in the production of concrete, both in the replacement of cement – larger consumption – and in the substitution of the natural fine aggregates, has been widely presented as a suitable solution for the reduction of this waste [4].

Bottom ash (BA) has also been targeted in some publications for its use in concrete and mortar [5–9].

The most important properties of BA are the size and shape of the particles and the porosity. Such properties depend on the burning efficiency, the method in which the BA is obtained and the type of combustion. When very small molten and well vitrified particles around 30 μm are formed, this satisfies the basic requirements of a fine aggregate for concrete and mortar, even if grain size distribution varies. There is also pozzolanic potential, although this is low due to the grain size [5].

The low pozzolanic potential of BA is not a limiting factor for its use as a fine aggregate, since any positive influence caused by the pozzolanic effect improves the mechanical performance and durability, due to calcium hydroxide consumption and formation of calcium silicate hydrate (C-S-H), which can be seen as a positive contribution of the BA [10,11].

However, to use BA as a raw material for concrete and mortar it is necessary to pay due attention mainly to the dosage parameters, for example, to the water/cement ratio [6]. This parameter is directly influenced by the hygroscopic characteristic of the BA and is difficult to control, since it is dependent on the raw material and the burning process, on the dimension of the particles and on the residue being extracted through a process involving a humid system.

Thus, BA will influence many properties: 1. water requirement, because of the fineness, the unburned material and the natural moisture content which is retained internally [1]; 2. filler effect, with an improvement in the filling role [6,10–13]; 3. mechanical properties, due to the pozzolanic effect, which stimulates the consumption of calcium hydroxide and the formation of C-S-H, which contributes to the filling of voids [10,12].

Furthermore, since BA has a high capacity for water retention, this feature must be considered in the evaluation of concrete produced with this by-product for use in water reservoirs [14].

* Corresponding author. Tel.: +55 4833315169; fax: +55 4833319272.
E-mail address: ecv1jcr@ecv.ufsc.br (J.C. Rocha).

0008-8846/$ - see front matter
doi:10.1016/j.cemconres.2006.11.001

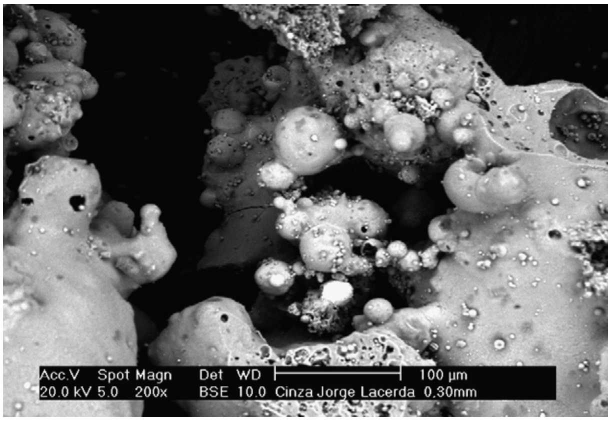

Fig. 1. SEM of bottom ash (ϕ<250 μm).

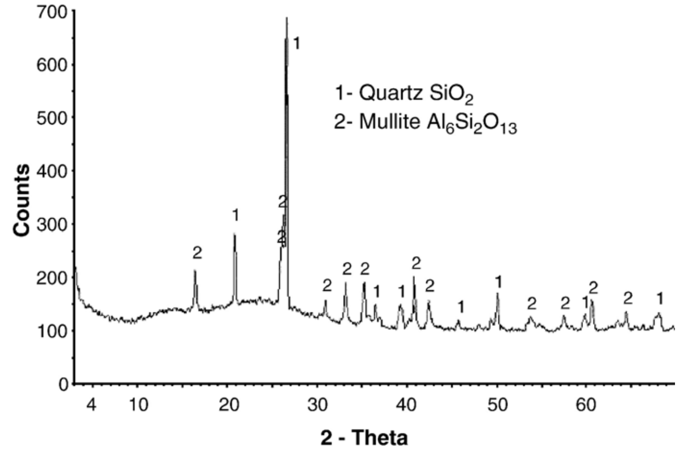

Fig. 2. X-ray diffraction analysis of bottom ash.

The moisture kinetics were studied in order to find a suitable selection of BA as a fine aggregate, with a view to gaining a better understanding of the characteristics of BA, considering it as a granular material like natural sand.

In this context, this paper reports on the effect of the moisture kinetics of BA as a granular material with an aggregate function and also evaluates the performance of concrete using BA as a natural sand replacement. The evaluation will be carried out using test methods to measure the capillary absorption and the water loss during air drying in tests with granular blends and concrete with bottom ash as a partial or total natural sand replacement.

2. Materials

The bottom ash used was collected from the Jorge Lacerda thermoelectric power station pond, Santa Catarina, southern Brazil, where 840 million tons of ash are available annually (Fig. 1). It has a specific gravity of 1.67 g/cm^3 and fineness modulus of 1.55. The BA was used in the concrete with its natural moisture content (55%), without previous oven drying. The bottom ash was collected and maintained in polypropylene bags and HDPE containers until the concrete production, to ensure the same water content. CP V Portland cement was used—ARI (high-early strength Portland cement), according to Brazilian standard NBR 5733/91 (similar to type III ASTM C150-05). The natural fine aggregate was river sand (NS) with a specific gravity of 2.63 g/cm^3 and fineness modulus of 2.50. The specific gravity of the natural coarse aggregate was 2.70 g/cm^3 and the maximum diameter was 19.0 mm.

The chemical and physical characteristics of the cement and the BA are shown in Table 1. In the chemical analysis of the BA particles, using X-ray dispersion spectrometry (XDS/Shimadzu), it was observed that approximately 78% of the material was composed of silica and alumina. The X-ray diffraction analysis (Fig. 2) indicates that the BA is comprised mainly of quartz and mullite.

Mixtures were made with bottom ash as a natural sand replacement (BA/NS) for analysis of the BA influence on the grain size distribution, as shown in Table 2.

In this paper, the assessment of the action of bottom ash as a fine aggregate involved the following procedures:

– elaboration of natural sand and BA blends;
– evaluation of the absorption by capillarity of the blends in terms of time;
– evaluation of the moisture kinetics of the drying of the blends.

Table 1
Chemical and physical characteristics of Portland cement and bottom ash

Content (%)	Cement	Bottom ash
Chemical analysis		
SiO_2	18.13	50.46
Al_2O_3	4.28	28.35
Fe_2O_3	2.54	10.69
K_2O	–	3.81
CaO	59.80	2.07
TiO_2	–	1.57
SO_3	3.14	0.34
ZrO_2	–	0.18
V_2O_5	–	0.09
MnO	–	0.07
ZnO	–	0.03
Y_2O_3	–	0.03
SrO	–	0.03
MgO	5.25	–
CaO free	1.47	–
Loss on ignition	3.29	2.3
Physical tests		
Blaine (cm^2/g)	4.098	–
Start of setting (h:min)	1:30	–
End of setting (h:min)	2:37	–
Specific gravity (g/cm^3)	3.12	1.674

Table 2
Grain size distribution of some of granular material compositions

Blend	Sand — NS (%)	Bottom ash — BA (%)	Grain size distribution (%)		
			<250 μm	250 — 500 μm	>500 μm
0% BA/NS [a]	100	0	19.0	21.0	60.0
25% BA/NS	75	25	22.0	26.0	52.0
50% BA/NS	50	50	28.0	22.0	50.0
75% BA/NS	25	75	36.0	24.0	40.0
100% BA/NS	0	100	50.0	28.0	22.0

[a] Reference granular sample.

Table 3
Mix proportion and concrete properties

Concrete type										
Mix proportion Kg/m^3		0% CRT	25% CRT3	50% CRT3	75% CRT3	100% CRT3	25% CRT4	50% CRT4	75% CRT4	100% CRT4
Cement		304	305	301	295	299	323	334	356	386
Natural sand		912	686	452	221	0	727	501	267	0
Bottom ash		0	145	287	422	570	103	212	340	441
Coarse aggregate		806	808	798	782	792	856	885	943	1023
Water		219	277	336	373	378	245	272	303	323
Density* (Kg/m^3)	Fresh	2238	2177	2090	1964	1869	2220	2138	2109	2040
	1 day drying	2220	2157	2052	1927	1815	2197	2128	2092	2004
	28 days drying	2170	2077	1952	1768	1625	2131	2051	1991	1888
Compressive strength* (MPa)	3 d	15.9	12.5	9.9	6.3	4.2	19.5	17	16.1	21.2
	28 d	28.4	23.2	18	11.5	8.6	27.2	28.5	26.1	32.6
	90 d	32	25.7	23	14.9	12.5	32.1	35.9	32.7	38.4
Elastic modulus* (GPa)	3 d	17.1	14.8	10.3	8.3	7.1	19.7	18	16.8	17.5
	28 d	25.8	22.1	19.2	12.6	8.9	24	22.8	22.7	21.2
	90 d	26.1	26	23.8	19.1	11.6	27.4	27.3	25.2	26.9

*Note: Each test result is the average of tests on three sample specimens (100×200 mm cylinders).
0% CRT — reference concrete sample.

For the composition of the concrete mix proportions two different dosage schemes were used in order to test the influence of natural water content in the bottom ash at the time of concrete production: one considering the natural water content – CRT3; and the other discounting the natural water content, considering all contents (bottom ash+natural moisture) as solid material, with the aim of obtaining the same compressive strength in relation to the reference sample – CRT4. These concrete mix composition differences are due to the significant difference between the specific gravities of bottom ash and natural sand, which are responsible for the differences in the results for the water/cement ratio and in the cement content for each mix proportion [1,15].

The compositions of the two concrete types and of the contents of the bottom ash as a substitute for natural sand are given in Table 3. The concrete mix was prepared according to the conditions of commercial concrete production.

3. Action mode of bottom ash as an aggregate (granular material)

3.1. Capillary absorption

The samples were tested in a 10 cm diameter metallic ring, 4 cm high (Fig. 3), and the amount of capillary water absorbed was monitored using a graduated Mariote bottle (hydraulic gradient of zero). The BA and NS contents used in the blends and the specific gravity are shown in Table 4.

From the results, one can observe that the potential for water absorption of the BA is much higher than that of the natural sand. This fact is more evident the higher the BA content in the blend.

The increase in the final moisture content in relation to the increase in BA content in the blend, was linear. The same occurred with the porosity of the natural sand+bottom ash system. The results show that an increase in the calculated

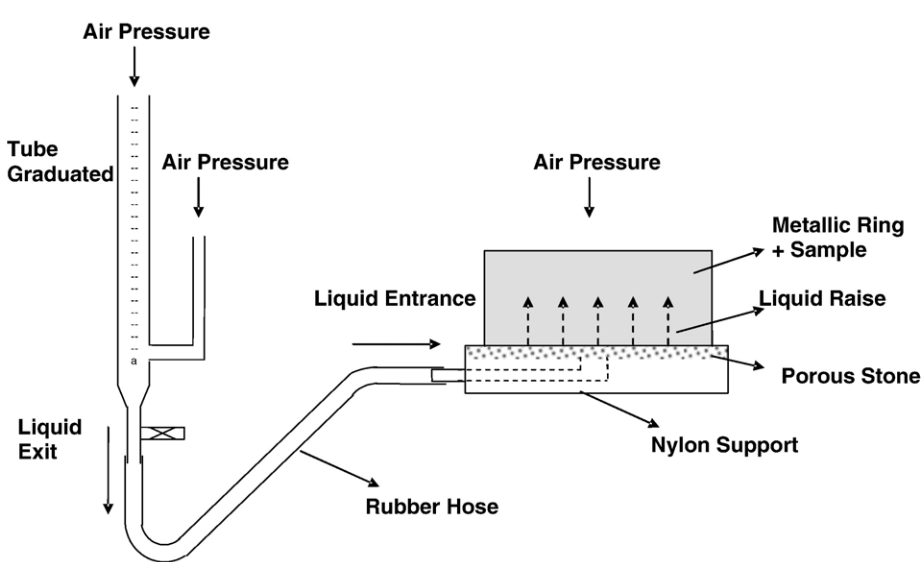

Fig. 3. Schema of test apparatus for capillary absorption — granular material.

Table 4
Compositions of natural sand and bottom ash

Sample	Material content, by weight (%)		Material content, by volume (%)		Final moisture system (%)	Unit weight (Kg/cm^3)	Specific gravity (Kg/cm^3)	Porosity	Sorptivity (g/cm^2/√s)	Total uptake water (g)
	Sand	BA	Sand	BA						
M1	100.0	0.0	100.0	0.0	21.3	1.515	2.634	0.425	0.058	121
M2	96.2	3.8	90.7	9.3	25.5	1.418	2.573	0.449	0.059	130
M3	91.6	8.4	81.0	19.0	29.7	1.322	2.508	0.473	0.058	136
M4	85.9	14.1	70.4	29.6	33.8	1.235	2.467	0.500	0.079	146
M5	80.8	19.2	62.1	37.9	39.0	1.126	2.405	0.532	0.106	155
M6	74.1	25.9	52.7	47.3	46.1	1.023	2.308	0.557	0.103	167
M7	64.4	35.6	41.4	58.6	54.4	0.941	2.232	0.579	0.126	178
M8	39.1	60.9	20.1	79.9	75.0	0.774	2.066	0.625	0.165	202
M9	0.0	100.0	0.0	100.0	82.0	0.591	1.814	0.674	0.158	223

porosity represents the potential for greater capillary absorption. However, in granular materials that contain BA, it is not only the voids between the particles which generate capillary absorption. There is also the influence of the absorption of the BA particle itself, i.e., its intrinsic porosity, the porosity of the particle.

An increase of 50% in the porosity of the sand + BA system makes the final moisture content almost triple. This demonstrates that not all of the water absorbed due to the increase in porosity is found in the additional interparticle voids. Part of it migrates to the interior of the BA particles, thus generating a very high level of final moisture in the samples with BA, in relation to the reference sample (100% natural sand).

There is, however, still the influence of the grain size to consider. BA has many particles, which are smaller than 0.15 mm, which increases the specific surface of the system, resulting in a larger amount of liquid to wet the particles, i.e., the water adsorbed on the surface. However, this factor is not so significant, since the amount of particles which are less than 0.15 mm is below 25% for a system with 100% of BA content (for the reference sample the total is 9%). This means that for lower BA content, the percentage of material which filters through a 0.15 mm sieve decreases. For example, for 50% BA (in volume), 16% of the material is smaller than 0.15 mm.

Due to the low specific gravity value for the BA particle, the results for absolute specific gravity and the unit weight of the blends undergo significant reductions, of up to 31% for the specific gravity and up to 61% for the unit weight.

For the range of BA content studied there was a significant water absorption variation of up to 40%. This fact is due to the low BA content that does not exert a significant influence on the increase in water absorption.

The water fixation potential and the capillary absorption kinetics are evaluated through the absorption index "I", shown in Fig. 4, which relates to time. This index is calculated relating the mass of liquid infiltrated to unit area of sample in contact with the liquid.

It can be seen that the final absorption index increases steadily with the increase in BA content. This indicates that the potential for capillary absorption is strongly influenced by the BA content in the blend and the absorption index value is dependent on the proportion of BA added. For the sample with 100% BA the increase in the absorption index reaches 85% of the reference sample value.

Fig. 4 shows that the presence of bottom ash has a significant influence on the behavior of the capillary absorption kinetics. With an increase in the BA content in the blended sample, the slope in the curve of the absorption over the square root of time becomes greater, and the higher the BA content in the blends, the faster the capillary absorption velocity.

The slope of the curve where there is proportionality, i.e., the linear part, supplies the data to calculate the sorptivity [16].

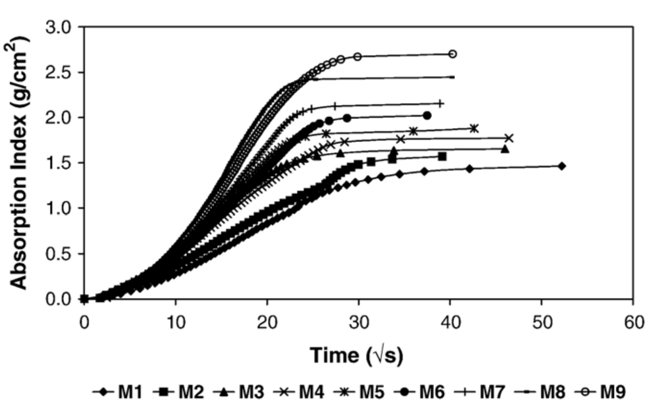

Fig. 4. Water absorption by unit area — granular material.

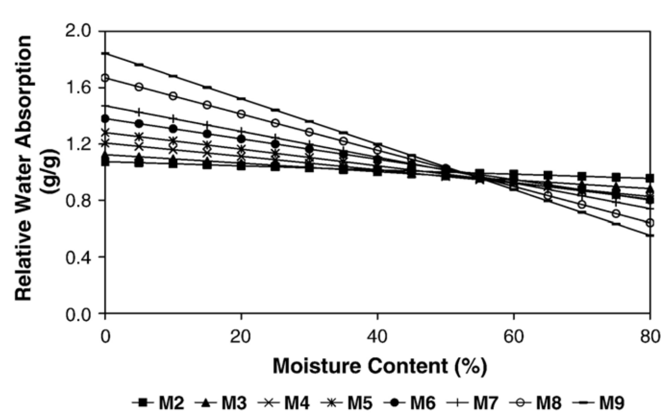

Fig. 5. Water absorption potential in relation to reference sample and bottom ash moisture content — granular material.

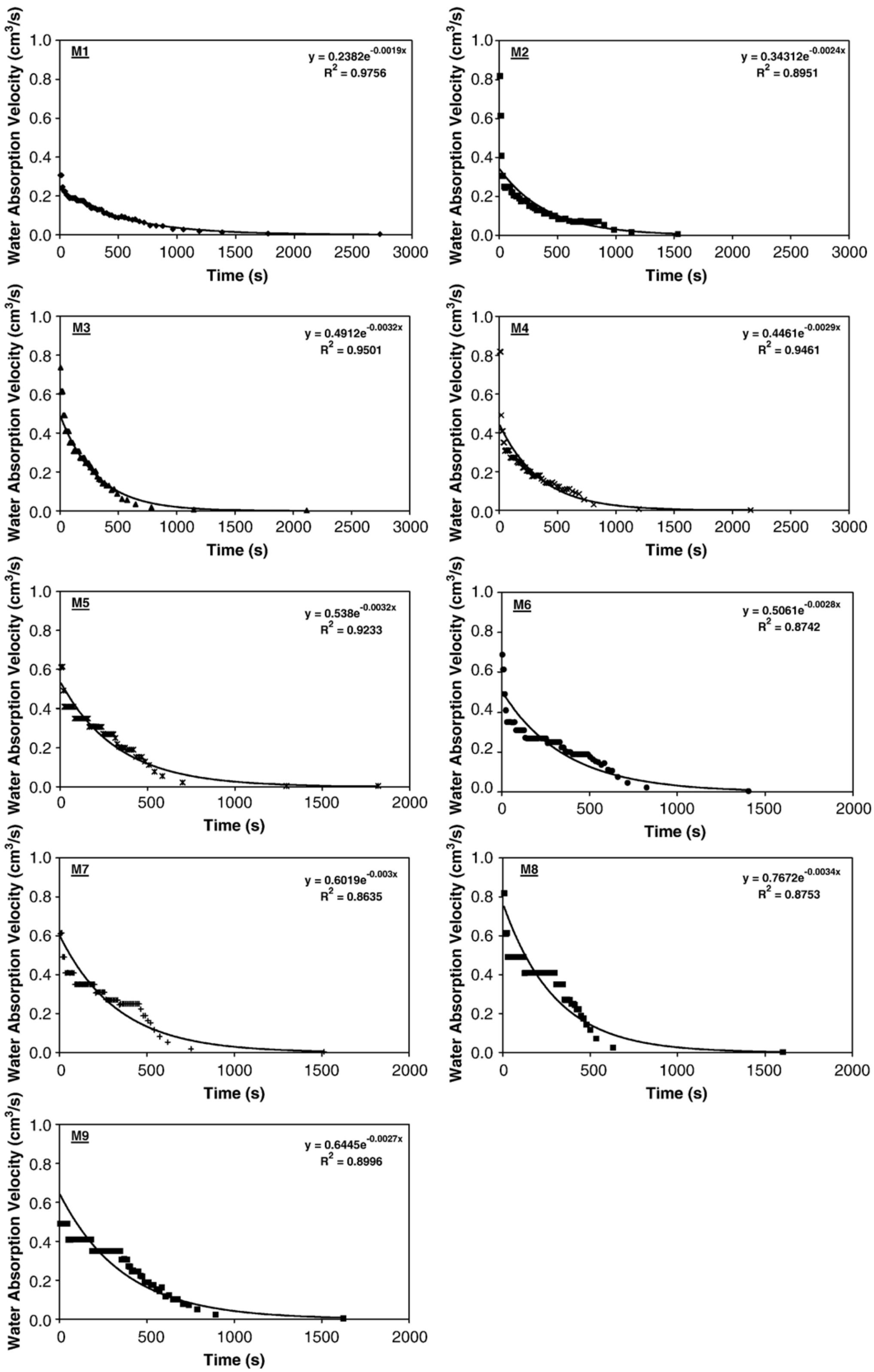

Fig. 6. Water absorption kinetics — granular material.

Since the samples with BA tend to form systems with higher absorption indexes and also with higher absorption rates, the sorptivity coefficients increase significantly when the BA content is increased. This means that the composite systems that contain bottom ash absorb, through capillarity, higher amounts of liquid (higher index of final absorption) in less time (higher rate of absorption) and can reach results two to three times higher than those for the natural sand sample.

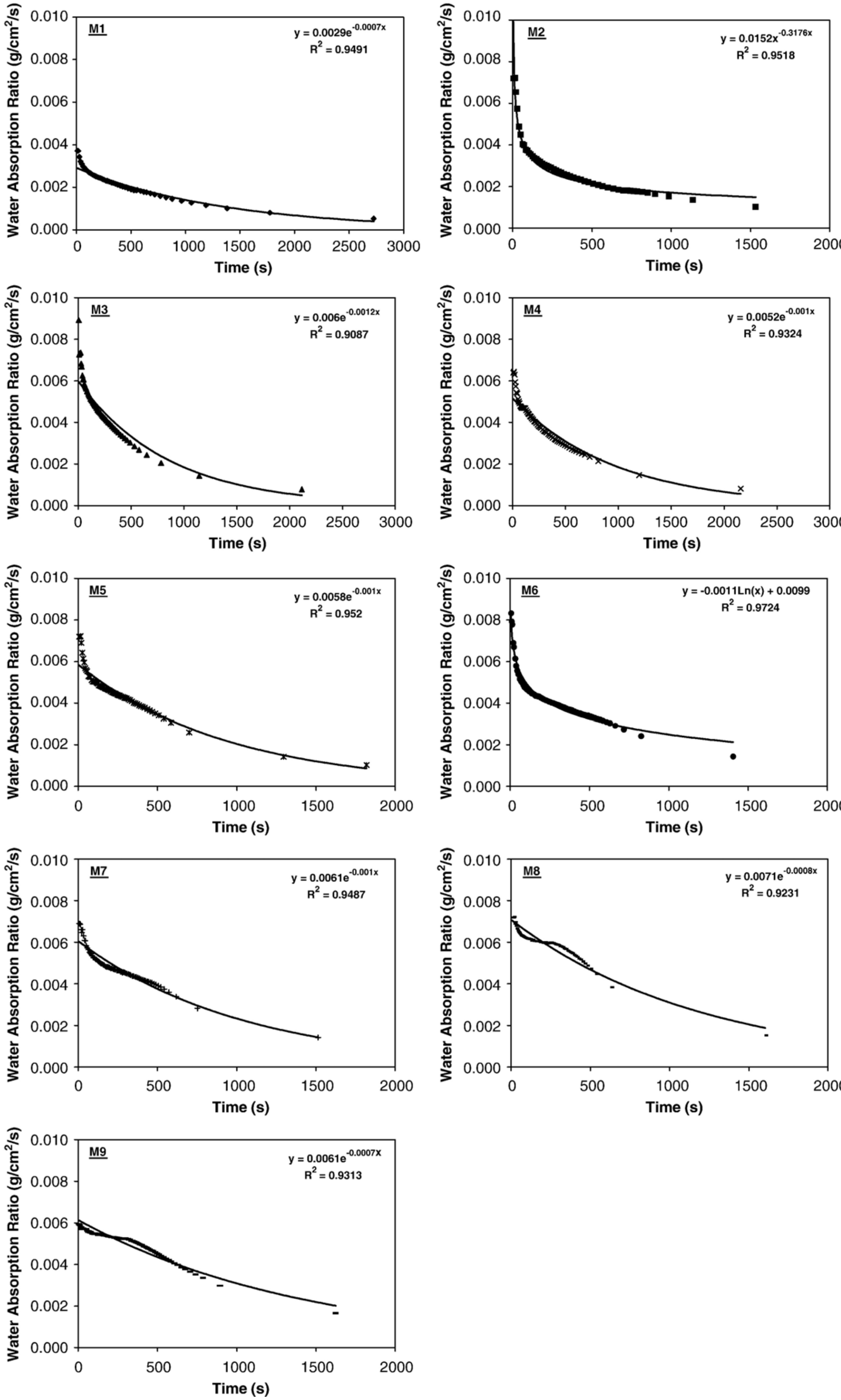

Fig. 7. Water absorption rate in relation to contact time — granular material.

The use of numerical simulation became necessary in this study, since the BA particles have a porosity that influences the capillary absorption in the experiment with granular material. This simulation was used to analyze the influence of the presence of natural moisture in the BA at the moment of the test, for each BA content investigated, modifying the initial bottom ash moisture content and calculating the amount of water absorbed by the blend.

The numerical simulation was carried out aiming to save time and to reduce the number of tests on the effect of the incorporation of bottom ash on the capillary absorption of water, when the surface moisture and the porous aggregate moisture absorption are varied.

The calculations were carried out varying the bottom ash moisture content (since the experiment was carried out with bottom ash dried in an oven) for each sand/BA mix. The calculations of the simulation were carried out using the Eq. (1) below:

$$\mathrm{Abs} = V_{\mathrm{H2O}_x} \cdot \left(m_{\mathrm{czp}_x} * \frac{h}{100} \right) \tag{1}$$

Abs calculated quantity of absorbed water, in g
V_{H2O} volume of absorbed water in the test with bottom ash moisture content equal to 0, in g
M_{BA} bottom ash mass in the sand/BA mix, in g
h moisture content, in %
x corresponding sample

Fig. 5 shows this numerical simulation, which considers the amount of water necessary to wet the bottom ash particles to a determined value of moisture content as a percentage of material weight, in relation to BA content.

The results of the numerical simulation show that there is a linear relation between the BA moisture content and the amount of water absorbed by the blend in relation to the reference sample with natural sand.

This confirms the previous findings that the influence of the BA content on the behavior of the capillary absorption is very significant. At 100% BA content in the replacement material, the moisture is above 80%. For moisture contents of approximately 50%, in terms of weight, the amount of water absorbed through capillarity is practically the same as the amount absorbed by the reference sample. This supplies important information for estimates of water content in concrete and mortar with bottom ash.

Another important parameter to be considered is the quantity of water absorbed for high values of natural moisture. For a bottom ash moisture content of 80%, the quantity of water absorbed in the sample of 100% BA was approximately 60% of the total quantity absorbed by the reference sample. This indicates that it absorbed lower amounts of water than the sample with 100% natural sand.

Figs. 6 and 7 show all of the considerations which have been discussed in the previous paragraphs. These figures show the relationship between time and absorption velocity and absorption ratio. One can see that with the increase in BA content, there is an increase in the absorption velocity and the absorption rates, and the greater the BA content the greater the increase in these values.

3.2. Water loss from air drying

Through the analysis of the water loss through air drying, the release of water from the BA/NS samples made up of granular

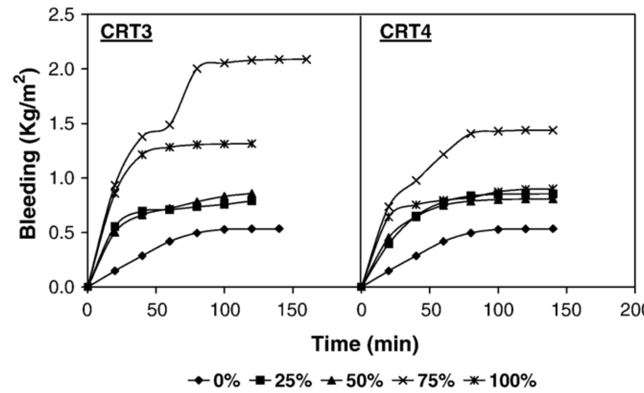

Fig. 9. Water loss through bleeding.

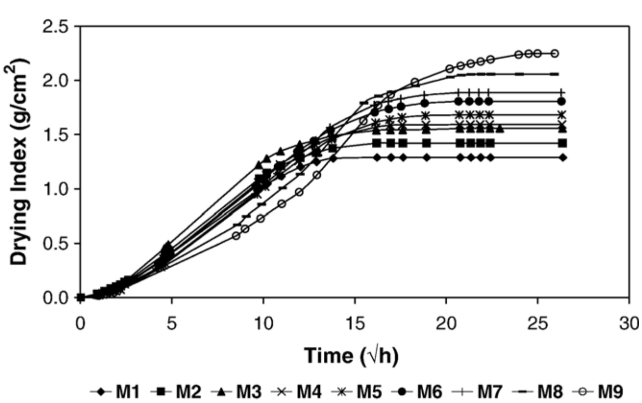

Fig. 8. Water loss by unit area over the square root of time — granular material.

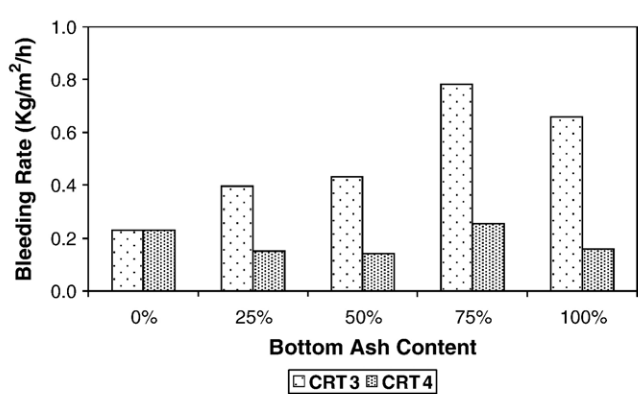

Fig. 10. Rate of water loss through bleeding in relation to concrete type and bottom ash content.

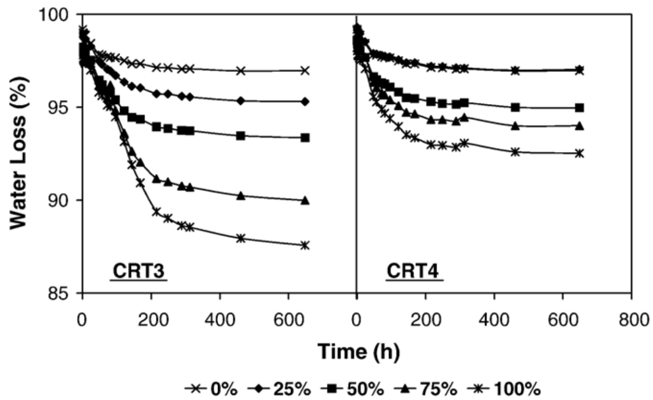

Fig. 11. Kinetics of water content loss though air drying of concrete in relation to the sample weight over time since molding.

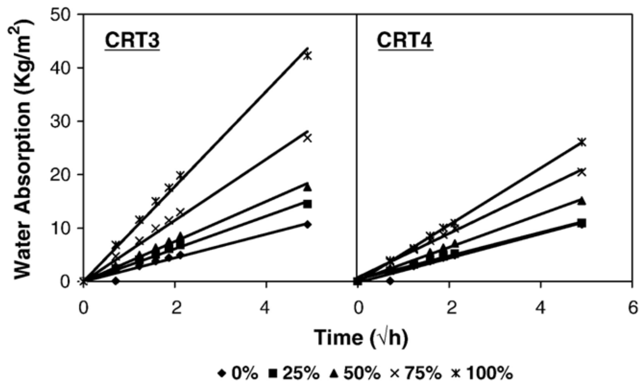

Fig. 13. Water capillarity absorption of concrete over the square root of time.

molded material in a standardized size metallic ring was investigated.

For environmental conditions where temperature is 22±2 °C and relative humidity is 60±5%, the phenomenon of water loss from air drying until a hygroscopic equilibrium was reached was observed, as shown in Fig. 8.

As in the case of the capillary absorption, the water loss from air drying was strongly influenced by the BA in the system. The higher the BA content the higher the water consumption and, consequently, the greater the water loss before a hygroscopic equilibrium was reached between the samples and the environment. However, the velocity of water loss from air drying did not differ greatly between the reference sample and the samples with BA and the slopes of the rectilinear part of the curves of the drying index "DI" were very similar.

4. Action mode of bottom ash in concrete

4.1. Bleeding

The test for water loss from bleeding was carried out using a glass mold, in which a sample of fresh concrete filled a surface area of 140×190 mm. The water quantity loss by bleeding was measured in terms of time. The end of the test was taken as time "*t*", when it was no longer possible to collect water from the surface of the sample. The experiment was carried out in a chamber where the temperature was 22±2 °C and the relative humidity, 60±5%.

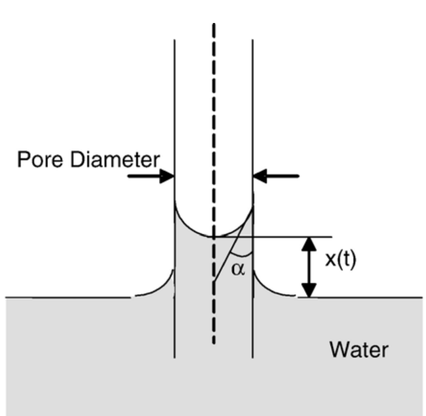

Fig. 12. Action of water transportation through capillarity in a concrete pore.

The results for the total water loss were close for the two types of concrete: CRT3 and CRT4. However, it was noted that this loss was greater the higher the BA content, due to the total amount of water in the mixes, which increases with increasing BA content.

As seen in Fig. 9, the times needed for most of the water to be lost through bleeding were similar for the two types of concrete. In the case of the reference mix, the curve stabilized after 80 min. For concrete samples with 100% BA, as the substitute material for sand, this value was noted for the two types. For the other concrete samples which were comprised of 25% BA, 50% BA and 75% BA, the time "*t*" was 60 min.

The bleeding rate measured, which is shown in Fig. 10, confirms the comments referring to Fig. 9, where a higher water loss rate was observed for higher BA content. The highest rates were obtained for the CRT3 concrete type.

4.2. Water loss through air drying

In the tests for water loss through air drying the samples were cast in metallic cylindrical molds of 100×200 mm (diameter×height). The moisture loss measurements were carried out by weighing the samples, after demolding, and the weight difference related to the water lost during this period. Since the exposure environment is a factor that significantly influences the results, each concrete sample was placed in a room with constant temperature and relative humidity of 22±2°C and 60±5%, respectively. The weights of the samples were determined over a period of 28 days.

Table 5
Sorptivity coefficient for the water and alcohol test on bottom ash concrete

Sorptivity coefficient ($Kg/m^2/h^{1/2}$)										
Concrete	Water test					Alcohol test				
	0%	25%	50%	75%	100%	0%	25%	50%	75%	100%
CRT3	2.2	3.1	3.8	5.7	8.9	1.1	1.4	1.8	2.8	4.0
CRT4		2.3	3.2	4.4	5.3		1.2	1.4	1.9	2.2

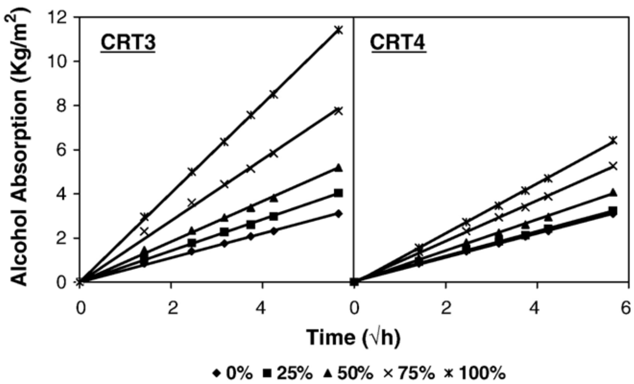

Fig. 14. Alcohol capillarity absorption of concrete over the square root of time.

Cementitious materials need a certain level of water content for hydration and a composite formation that will give mechanical strength and durability when exposed to aggressive agents, along with an additional quantity of water so that the concrete will have rheological characteristics which lead to workability, consistency and the desired fluidity.

Fig. 11 shows that the variation in the results is due to the moisture state of the samples, that is, the higher the quantity of water in the concrete the higher the amount of water lost through air drying. The figure also shows that concrete with a higher BA content gave higher losses of water from drying.

Due to the increase in the connectivity and high water/cement (w/c) ratio, which are factors that lead to high values of water loss through air drying, it can be concluded that the increase in bottom ash content contributes to a better connection between capillary pores. This is confirmed by the results obtained in the capillary absorption tests.

4.3. Capillary absorption

The same samples used for the air drying test were used for the capillary absorption test and these had been cured over a period of 28 days, in a controlled environment. After this period the samples were placed in an oven at 50 °C for forced drying to remove the remaining water from the samples.

As with the air drying test, the data collected in the capillary absorption experiment were used to measure the mass increase of the sample from liquid absorption, from which the sorptivity coefficient is calculated [18]. The apparent wetting contact angle (α), see Fig. 12, was determined using two different penetrating liquids: water, as the main liquid, and alcohol with perfect wettability, i.e., liquid–solid contact angle of 0°.

Fig. 13 shows the strong influence that the bottom ash has on the capillary distribution. This is due not only to the significant increase in the final w/c ratio when the BA content is increased, but also to the increase in the BA content itself, which generates a different capillary configuration to the reference mix.

It is known that an increase in total water content tends to form a system in which part of this water will be present as free water and, consequently, the system will have a greater porosity.

However, it is known that when cement hydration begins, a reduction in the internal water content is initiated, as this water becomes part of the hydrates, as chemically added water, and begins to be lost through bleeding and evaporation, these being common phenomena which are dependent on the environment and the characteristics of the mixture.

Thus, an increase in the water quantity of a mix leads to an increase in the quantity of water that is lost, and consequently, an increase in the value of the capillary absorption for this mix.

On analyzing the contents studied, it can be seen that only the 25% CRT4 has a result similar to that obtained for the reference mix, and all the others are close, or show higher values.

In accordance with the aforementioned explanations, the presence of BA in the mix does not influence the increase in capillary absorption of concrete, and one must not conclude that the increase in the final w/c ratio (due to the initial moisture condition) is the only factor determining the differences. What is actually occurring is a significant change in the capillary structure (size and connectivity of the pores).

Table 5 shows the sorptivity coefficient values obtained from concrete with BA content.

According to the analysis of the material characteristics, BA has a higher quantity of fine material than natural sand. Therefore, the greater the BA content the better the filling-of-voids effect will be from the fine particles of the incorporated BA content. Thus, mixtures with smaller pore sizes (diameter) tend to have a faster water absorption velocity through capillarity.

It can be concluded then, that with the increase in BA content the voids tend to be better filled, due to a decrease in the diameter of the pores in the concrete. On the other hand, since BA is an element that requires water through intrinsic internal absorption, it increases the quantity of water absorbed through capillarity.

There is the possibility of calculating the apparent wetting contact angle for the concrete using water and alcohol as penetrating liquids, according to the experiment described by Merouani [17].

The study on capillary absorption using alcohol as a penetrator fluid, gave lower results than the tests carried out with water, as shown in Fig. 14.

Table 6
Constant characteristics of capillary absorption fluids (T=20 °C)

Liquid	σ (dynes/cm)	μ (centipoises)	ρ (g/cm^3)
Water	72.75	1.005	1
Alcohol	23.04	1.2	0.789

Table 7
Apparent wetting contact angle of bottom ash concrete

Concrete	BA	Apparent wetting contact angle α_e
	0%	49°
CRT3	25%	40°
	50%	46°
	75%	46°
	100%	37°
CRT4	25%	47°
	50%	35°
	75%	22°
	100%	21°

Table 6 shows the apparent wetting contact angles obtained for BA concrete, using water and alcohol. Since the apparent wetting contact angle has an inversely proportional relation with the slope of the curve for the menisci position over a certain time period, the small apparent contact angles characterize better wettability. This means that mixtures with larger apparent wetting angles tend to have a more advanced capillary front; however, they have less infiltrated liquid.

For the calculation of the apparent wetting contact angle, Eqs. (2) and (3) were used. Table 7 gives the constants for the calculations of Eqs. (2) and (3).

$$\cos\alpha_e = \left(\frac{S_e}{S_a}\right)^2 \frac{\mu_e \times \sigma_a}{\mu_a \times \sigma_e} \quad (2)$$

Where,

α_e apparent wetting contact angle (°);
μ_e dynamic viscosity of water (centipoises);
μ_a dynamic viscosity of alcohol (centipoises);
σ_e superficial tension of water/air (dynes/cm);
σ_a superficial tension of alcohol/air (dynes/cm);
S_e slope of the straight line of the graph which relates to water absorption (St) versus the square root of time (cm);
S_a slope of the straight line of the graph which relates to alcohol absorption (St) versus square root of time (cm).

$$S(t) = \frac{m(t) - m_s}{\rho_1 \times A} \quad (3)$$

Where,

$S(t)$ quantity of infiltrated liquid (cm);
$m(t)$ weight of the sample at a specific moment (g);
m_s weight of the sample dried in an oven (g);
ρ_1 density of the liquid used (g/cm^3);
A cross sectional area of sample = 78.540 cm^2.

5. Conclusions

The following conclusions can be drawn from this research:

- The potential for capillary absorption of granular materials was greater when bottom ash (BA) was present in the system. Also, the greater the BA content the higher the absorption. However, this increase in the capillary absorption of the natural sand + bottom ash blend was not a direct result of an increase in the number of small particles, but was the result of the porosity of the bottom ash particles which directly influenced the increase in water content due to the migration of quantities of water from the BA. This can be proven by the test method used in this study.
- The absorption index "*I*" was 85% higher in the sample with 100% of bottom ash in relation to the reference sample which was composed of only natural sand. The absorption velocity was also higher in the BA/NS blends and in the sample with only bottom ash. Due to this, the sorptivity increased when the BA content increased, reaching a three-fold increase with a quantity of 100% BA in relation to the reference sample. When the bottom ash that was added to the blends of granular material contained some moisture, considered in this paper through numerical simulation, the quantity of absorbed water was less. At 50% levels of humidity, the quantities absorbed in the samples with bottom ash are similar to those absorbed in the reference sample.
- The fact that the bottom ash absorbed part of the water that was used in the capillary absorption study, suggests that this water has a great potential for being released in the same way as it is absorbed. This can be seen in the study on water loss through air drying or hygroscopic equilibrium. For all the cases – M1…, M9 – the samples went through the process of almost totally drying out, leading us to believe that all the water that is absorbed by bottom ash tends to subsequently leave it.
- The tests carried out with the presence of bottom ash (BA) as a fine porous aggregate with a high potential for water absorption, indicate that the parameters relating to water transport behavior – bleeding, moisture equilibrium from air drying, absorption from capillarity, sorptivity – are greatly affected in relation to those for normal concrete.
- In relation to the study on water loss from bleeding, it can be concluded that the higher the quantity of water in BA concrete, the higher the amount of water lost through bleeding, since BA concrete has a lesser capacity of water retention. The fact that the CRT4 concrete had less BA in its composition in relation to the total weight of the concrete did not change this performance, even though lower values were obtained than those for the CRT3 concrete.
- With reference to the water loss from air drying, it can be seen that the quantity of water which was present in the concrete, was the most important factor for the increase in lost water. Comparing the CRT3 and CRT4 mix proportions, it can be noted that the concrete type 3, was the one which lost the most moisture, because of the higher water content in relation to CRT4.
- Capillary absorption potential of the fine aggregates of the concrete was higher when there was bottom ash in the system. Also the absorption was higher, the higher the BA content which was incorporated. In the case of the CRT4 concrete the results for the apparent wetting contact angles show a decreasing trend when the BA content was increased. The bottom ash has a greater quantity of fine particles in relation to the natural sand. For this reason, the greater the bottom ash content the better will be the effect of the filling role by the fine particles of the bottom ash incorporated.

References

[1] N. Ghafoori, J. Bucholc, Investigation of lignite-based bottom ash for structural concrete, J. Mater. Civ. Eng. 8 (3) (1996) 128–137.
[2] N. Ghafoori, J. Bucholc, Properties of high-calcium dry bottom ash concrete, ACI Mater. J. 94 (2) (1997) 90–101.
[3] O.E. Manz, Worldwide production of coal ash and utilization in concrete and others products, Fuel 76 (1997) 691–696.
[4] D. Ravina, Properties of fresh concrete incorporating a high volume of fly ash as partial fine sand replacement, Mater. Struct. 30 (1997) 473–479.

[5] M. Cheriaf, J. Péra, J.C. Rocha, Pozzolanic properties of pulverized coal combustion bottom ash, Cem. Concr. Res. 29 (1999) 1387–1391.
[6] L.B. Andrade, Methodology of assessment to use of bottom ash of thermoelectric power plants as aggregate in concrete (M.Sc. Thesis), Department of Civil Engineer, Federal University of Santa Catarina, Santa Catarina, Brazil, 2004. (in Portuguese).
[7] L.B. Andrade, J.C. Rocha, M. Cheriaf, Performance of concrete mortar with bottom ash as fine natural aggregate replacement, Proceedings of Conference on Sustainability Development and Recycling in Civil Construction — Recycled Materials and its Applications, São Paulo: Ibracon — Technical Committee, vol. 206, 2003. (in Portuguese).
[8] L.B. Andrade, J.C. Rocha, M. Cheriaf, Study of use of coal bottom ash of thermoelectric as fine aggregate in concrete, Proceedings of 1° Latin–American Conference of Sustainable Construction and 10° National Meeting of Technology of Environment Built, São Paulo: ANTAC, 2004. (in Portuguese).
[9] A.L. Kreuz, M. Cheriaf, J.C. Rocha, Properties of structural concrete with bottom ash as partial sand replacement, Proceedings of Conference on Sustainability Development and Recycling in Civil Construction — Recycled Materials and its Applications, São Paulo: Ibracon — Technical Committee, vol. 206, 2001, pp. 215–224. (in Portuguese).
[10] S.P. Pandey, R.L. Sharma, The influence of mineral additives on the strength and porosity of OPC mortar, Cem. Concr. Res. 30 (2000) 19–23.
[11] Z. Chengzi, W. Aiqin, T. Mingshu, L. Xiaoyu, The filling role of pozzolanic material, Cem. Concr. Res. 26 (1996) 943–947.
[12] G.C. Isaia, A. Gastaldini, R. Moraes, Physical and pozzolanic action of mineral additions on the mechanical strength of high-performance concrete, Cem. Concr. Compos. 25 (2003) 69–76.
[13] I. Odler, M. Robler, Investigations on the relationship between porosity, structure and strength of hydrated Portland cement pastes. ii — effect of pore structure and of degree of hydration, Cem. Concr. Res. 15 (1985) 401–410.
[14] N. Barbare, A. Shukla, A. Bose, Uptake and loss of water in cenosphere–concrete composite material, Cem. Concr. Res. 33 (2003) 1681–1686.
[15] P.J. Wainwright, H. Ait-Aider, The influence of cement source and slag additions on the bleeding of concrete, Cem. Concr. Res. 25 (1995) 1445–1456.
[16] L. Hanzic, R. Ilic, Relationship between liquid sorptivity and capillarity in concrete, Cem. Concr. Res. 33 (2003) 1385–1388.
[17] L. Merouani, Phénomènes de sorption et de transfert d'humidité dans des matériaux du bâtiment. Étude expérimentale comparative d'un mortier de ciment et d'un enduit de façade. Thèse Docteur 3o Cycle. Institut National Polytechnique de Grenoble, 1987 (in French).
[18] C. Hall, Water sorptivity of mortars an concretes: a review, Mag. Concr. Res. 41 (1989) 51–61.